

rstb.royalsocietypublishing.org



Research

Cite this article: Shaver GR, Rastetter EB, Salmon V, Street LE, van de Weg MJ, Rocha A, van Wijk MT, Williams M. 2013 Pan-Arctic modelling of net ecosystem exchange of CO₂. *Phil Trans R Soc B* 368: 20120485. <http://dx.doi.org/10.1098/rstb.2012.0485>

One contribution of 11 to a Theme Issue 'Long-term changes in Arctic tundra ecosystems'.

Subject Areas:
ecology

Keywords:
Arctic carbon cycling, net ecosystem exchange of carbon, tundra, carbon cycle modelling, pan-Arctic comparisons

Author for correspondence:
G. R. Shaver
e-mail: gshaver@mbl.edu

Pan-Arctic modelling of net ecosystem exchange of CO₂

G. R. Shaver¹, E. B. Rastetter¹, V. Salmon^{1,2}, L. E. Street^{1,3}, M. J. van de Weg^{1,4}, A. Rocha^{1,5}, M. T. van Wijk^{6,7} and M. Williams⁷

¹Ecosystems Center, Marine Biological Laboratory, Woods Hole, MA, USA

²Department of Biology, University of Florida, Gainesville, FL, USA

³Department of Geography, University of Sheffield, Sheffield, UK

⁴Amsterdam Global Change Institute, Vrije Universiteit, Amsterdam, The Netherlands

⁵Department of Biological Sciences, University of Notre Dame, Notre Dame, IN, USA

⁶School of Geosciences, University of Edinburgh, Edinburgh, UK

⁷Plant Sciences, Wageningen Agricultural University, Wageningen, The Netherlands

Net ecosystem exchange (NEE) of C varies greatly among Arctic ecosystems. Here, we show that approximately 75 per cent of this variation can be accounted for in a single regression model that predicts NEE as a function of leaf area index (LAI), air temperature and photosynthetically active radiation (PAR). The model was developed in concert with a survey of the light response of NEE in Arctic and subarctic tundras in Alaska, Greenland, Svalbard and Sweden. Model parametrizations based on data collected in one part of the Arctic can be used to predict NEE in other parts of the Arctic with accuracy similar to that of predictions based on data collected in the same site where NEE is predicted. The principal requirement for the dataset is that it should contain a sufficiently wide range of measurements of NEE at both high and low values of LAI, air temperature and PAR, to properly constrain the estimates of model parameters. Canopy N content can also be substituted for leaf area in predicting NEE, with equal or greater accuracy, but substitution of soil temperature for air temperature does not improve predictions. Overall, the results suggest a remarkable convergence in regulation of NEE in diverse ecosystem types throughout the Arctic.

1. Introduction

Arctic landscapes consist of a diverse patchwork of ecosystem types, often with sharply defined borders between ecosystems that differ greatly in key processes of C cycling such as gross primary production (GPP), ecosystem respiration (R_E) and net ecosystem exchange (NEE) of CO₂ [1]. The dominant species in the vegetation of these ecosystem patches may be herbaceous or woody; it may be deciduous, evergreen, wintergreen, graminoid, moss or lichen. The size of the patches as well as the frequency of the different kinds of patches also varies widely across the Arctic [2–4]. This high spatial variability makes it difficult to predict accurately the regional C balance and its overall change in response to weather and climate change. Models of pan-Arctic C cycling typically view the Arctic as consisting of only one or a very small number of ecosystem types, all responding to weather and climate in about the same way [5–7]. Yet the accuracy of this approach is not well tested, mostly because of a lack of information on similarities and differences in responses of different kinds of Arctic ecosystems to changes in weather across the full range of Arctic climates and landscapes. We still do not know how many kinds of tundra must be considered to model pan-Arctic C balance and predict future changes with acceptable accuracy [8].

In this paper, we continue development of a model of net CO₂ exchange (NEE) in Arctic ecosystems that is based on short-term measurements of the light response of CO₂ fluxes in whole canopies of tundra vegetation and the soils beneath them. We have already shown that this model can be used

with confidence to predict CO₂ fluxes across a wide array of subarctic and low Arctic ecosystems [9]. No knowledge of species composition is necessary to make these predictions; the model requires as inputs only (i) photosynthetically active radiation (PAR), (ii) air temperature, and (iii) leaf area per square metre ground (LAI derived from a measure of canopy reflectance, the normalized difference vegetation index, NDVI). The model is parametrized on the basis of local surveys of the light response of NEE in small plots (approx. 1 m²); it has also been used successfully to scale up to broad regions using satellite-derived NDVI [10].

Here, we develop the model [9] further in three ways, first by testing whether a single parametrization of the model can be used to predict NEE with acceptable accuracy over a wider latitudinal range, including both low and high Arctic sites. Second, we use canopy N content rather than leaf area to predict NEE. Foliar N is known to be correlated with carboxylation capacity and autotrophic respiration rates [11]. Finally, we evaluate the use of soil temperature rather than air temperature as a predictor of NEE. We expect heterotrophic respiration to be more closely linked to soil temperature [12]. The overall aim of this work is to find a single model and, ideally, a single parametrization of that model, that makes accurate predictions of NEE through the Arctic using information (air/soil temperature, irradiance and leaf area/foliar N) that can be obtained by remote sensing.

2. Material and methods

(a) Sites and sources of data

Most of the data used in our analysis have been used previously in different comparisons and for other purposes. Here, we combine these data in a pan-Arctic analysis, adding previously unpublished data from 2009 (table 1). The entire, combined dataset is available from the US Arctic Long-Term Ecological Research (LTER) project at <http://dryas.mbl.edu/arc/ITEX/data.html>.

All of the data come from surveys of the response of NEE to changes in light (PAR) that were completed in a wide range of subarctic, low Arctic and high Arctic ecosystems during the summers of 2003–2009. The five sites were

- Toolik Lake, Alaska, including three subsites accessible by walking, driving or helicopter from Toolik Field Station. These were (i) the research plots of the US Arctic LTER project [17], (ii) nearby Imnavait Creek [18], and (iii) the 2007 Anaktuvuk River (AR) Wildfire about 40 km north of Toolik Lake [19–21].
- Abisko, Sweden, including three subsites within 15 km of the Abisko Scientific Research Station [13,14]. These were ‘Paddus’, ‘Steps’ and ‘Latnjajaure’.
- Longyearbyen, Svalbard, including ecosystem types within the Adventalen valley [14].
- Zackenberg, Greenland, including ecosystem types within 2 km of the Zackenberg Ecological Research Station [14].
- Barrow, Alaska, including a ecosystem types within the Barrow Environmental Observatory [14].

For this analysis, we consider Toolik Lake and Abisko to be ‘low Arctic’ and Longyearbyen, Zackenberg and Barrow to be ‘high Arctic’. All five sites are above the Arctic Circle and have at least six to seven weeks of continuous darkness in winter and continuous light in summer. All are treeless except Abisko, where subarctic birch forest (*Betula tortuosa*; not sampled in this work) occurs at lower elevations. The mean annual air

temperature at all sites is less than 0°C and all but Abisko are underlain by continuous permafrost. The sites span 10° of latitude (68–78° N) and 10°C in mean annual temperature (–1 to –11°C). July mean air temperatures are 11–14°C at the two southernmost sites, and 4–6°C at the three northernmost sites. Toolik Lake lies within Bioclimatic Zone E as defined by the Circumpolar Arctic Vegetation Map [4], while Abisko is ‘subarctic’ by this classification. Longyearbyen, Zackenberg and Barrow are all within Bioclimatic Zone C.

At each site, the light response of NEE was described for the widest possible array of locally accessible ecosystem types, selected subjectively and distinguished by vegetation stature and composition. Although most of the plots selected were typical of local vegetation, effort was made to include extreme examples as well (e.g. high or low stature, dense or thin canopies, species-rich, monospecific or species-poor canopies). The dataset includes over 4800 individual measurements of NEE, as part of 448 light response curves from 247 individual plots (table 1). Most (greater than 90%) of the measurements were made within 2–3 h of solar noon, at the highest possible sun angles. We occasionally repeated the light response curves on some plots to help quantify the variability among repeated measurements. At Toolik Lake and Abisko, we also repeated measurements on some plots at different times during the growing season or at different times of day (e.g. every 4 h over 24–28 h). Most of the measurements were made in mid-July through early August, but in the present analysis, all data collected at any time during June–August, at any time of day, are included.

(b) Light response of net ecosystem exchange

At all sites, we measured NEE of CO₂ using a portable cuvette system as described in detail in Williams *et al.* [8] and Street *et al.* [13]. A clear Plexiglas cuvette was lowered onto a square aluminium base fitted with legs pushed into the soil to create a level support. The cuvette was sealed to the base by compression of a foam rubber gasket. A clear plastic skirt hung down from the base to the ground surface, and was sealed to the ground by draping a heavy chain on top of the skirt. This created an enclosed volume above each 1 × 1 m plot (at Zackenberg and Longyearbyen, we occasionally used a 30 × 30 cm base). The change in CO₂ concentration during each measurement was determined using a LI-COR 6400 or 6200 Photosynthesis System (LI-COR, Lincoln, NE, USA). NEE was calculated knowing the rate of change in [CO₂], the cuvette and base volumes, air temperature and barometric pressure. We assume that each measurement represents the net flux of CO₂ over the area of each plot (NEE), including GPP (or whole-canopy photosynthesis) and R_E (including both plant and soil respiration), where $NEE = R_E - GPP$.

We measured the light response of NEE by making a series of measurements on the same plot, starting with one to three measurements at full ambient light, followed by one or two measurements at each of several increasing levels of shading (usually three levels), followed by one to three measurements made in complete darkness. Shading was achieved by covering the cuvette and base with one to three layers of optically neutral shade cloth or mosquito netting, and the dark measurements were made by covering the system with an opaque tarp. Between measurements, the cuvette was ventilated by lifting it from the base and allowing CO₂ concentration to return to approximately the ambient value.

(c) Leaf area, canopy N content and environmental variables

Leaf area and the total amount of N in the canopy were estimated using established relationships with canopy reflectance, using the NDVI as the measure of reflectance [15]. Parameters for these regression relationships were established in separate

Table 1. Site information and sources of data. Classification by Bioclimatic Zone follows Walker *et al.* [3,4]. Numbers in rightmost column refer to: (1) Shaver *et al.* [9]; (2) Street *et al.* [13]; (3) Williams *et al.* [8]; (4) Street *et al.* [14] and (5) this study.

site	vegetation, Bioclimate Zone	latitude/longitude	annual, July mean temp.	no. canopy LAI, N harvests	subsite	years of measurement	no. plots	no. light response curves	no. NEE measurements	data sources
Toolik Lake, Alaska	low Arctic, Zone E	68°38' N, 149°36' W	-10°C, 14°C	94 ^a	Toolik LTER Innavait Creek Anaktuvuk River	2004, 2009 2003, 2004 2009	50 23 5	141 48 5	1571 679 52	1,2,4,5 3,4 5
Abisko, Sweden	low Arctic, (subarctic) Zone E	68°18' N, 18°51' E	-1°C, 11°C	92 ^a	Burn Strepps Paddus	2004, 2005 2004	53 13	112 13	1105 148	1,2,4 1,2,4
Longyearbyen, Svalbard	high Arctic, Zone C	78°13' N, 15°37' E	-5°C, 6°C	48	Longyearbyen	2005	41	41	473	4
Zackenbergl, Greenland	high Arctic, Zone C	74°28' N, 20°34' E	-9°C, 6°C	78	Zackenbergl	2006	47	59	609	4
Barrow, Alaska	high Arctic, Zone C	71°18' N, 156°40' W	-11°C, 4°C	23	Barrow Environmental Observatory	2009	13	13	157	4

^aIncludes earlier data from van Wijk & Williams [15] and Williams & Rastetter [16].

measurements of NDVI in undisturbed vegetation using a Unispec SC or DC Spectroradiometer (PP Systems, Amesbury, MA, USA), followed by harvest of the entire canopy within the field of view of the instrument (usually a circle approx. 20 cm in diameter) and determination of its leaf area and N content. Samples were collected from representative vegetation at all five sites (table 1). We estimated LAI ($\text{m}^2 \text{ leaf m}^{-2} \text{ ground}$) in all plots using the overall regression formula

$$\text{LAI} = 0.0026 \times e^{(8.0783 \times \text{NDVI})} \quad (r^2 = 0.736). \quad (2.1)$$

Similarly, canopy N content (N_T , g N in leaves $\text{m}^{-2} \text{ ground}$) was estimated as

$$\text{N}_T = 0.0471 \times e^{(4.995 \times \text{NDVI})} \quad (r^2 = 0.4021). \quad (2.2)$$

In addition to PAR and air temperature measurements that accompanied each measurement of NEE, for each light response curve, we also made four to six measurements of soil temperature at 5 cm depth using a digital soil thermometer. Additional measurements included estimates of plant cover by species and measurements of soil moisture using a Hydrosense soil moisture probe (Campbell Scientific, Logan, UT, USA); for many plots, we also measured soil temperature at the surface and at 10 cm depth and depth of soil thaw.

(d) Net ecosystem exchange model

The NEE model is identical to the NEE₂ model of Shaver *et al.* [9], where

$$\text{NEE} = R_E - \text{GPP}, \quad (2.3)$$

$$R_E = (R_0 \times e^{\beta T} \times \text{LAI}) + R_x \quad (2.4)$$

and

$$\text{GPP} = \frac{P_{\max L}}{k} \times \ln \frac{P_{\max L} + E_0 \times I}{P_{\max L} + E_0 \times I \times e^{(-k \times \text{LAI})}}. \quad (2.5)$$

The predicted NEE (equation (2.3)) is simply the difference between the R_E and GPP models ($\text{NEE} = R_E - \text{GPP}$); thus NEE is a negative value when CO_2 is removed from the atmosphere and positive when CO_2 is added to the atmosphere.

The respiration model (equation (2.4)) assumes that R_E comes from two sources. The first source produces CO_2 as a function of a basal respiration rate, R_0 ($\mu\text{mol CO}_2 \text{ m}^{-2} \text{ leaf s}^{-1}$), an exponential temperature response where β is an empirically fit parameter ($^{\circ}\text{C}^{-1}$) and T is air temperature ($^{\circ}\text{C}$) and LAI ($\text{m}^2 \text{ leaf m}^{-2} \text{ ground}$). This first source is assumed to account for the majority of R_E , including both autotrophic (plant) and heterotrophic ('soil') respiration. The Q_{10} for respiration of this pool can be calculated as

$$Q_{10} = e^{10\beta}. \quad (2.6)$$

The second source is a constant flux of CO_2 that is independent of LAI and air temperature. This was added to the model because it improves the accuracy of model predictions and the fit of the model to the data, and it prevents R_E from going to zero when there is no leaf area [9]. Other formulations were tested by Shaver *et al.* [9].

The GPP model (equation (2.5)) is an adaptation of the aggregated canopy photosynthesis model of Rastetter *et al.* [22], derived by applying the hyperbolic photosynthesis–light equation at the leaf level, using Beer's light extinction equation and integrating down through the canopy, where $P_{\max L}$ is the light-saturated photosynthetic rate per unit leaf area ($\mu\text{mol m}^{-2} \text{ leaf s}^{-1}$), k is Beer's law extinction coefficient ($\text{m}^2 \text{ ground m}^{-2} \text{ leaf}$) and E_0 is the initial slope of the light response curve or 'quantum yield' at low light ($\mu\text{mol CO}_2 \text{ fixed } \mu\text{mol}^{-1} \text{ photons absorbed}$).

In the present analysis, we also used canopy N content rather than LAI as a predictor of NEE, R_E and GPP. Doing this required substituting canopy N content (N_T , in units of g N m^{-2}

ground) for LAI in equations (2.4) and (2.5); this of course caused a change in units of $P_{\max L}$ (to $\mu\text{mol CO}_2 \text{ g}^{-1} \text{ N s}^{-1}$), k (to $\text{m}^2 \text{ ground g}^{-1} \text{ N}$) and R_0 (to $\mu\text{mol CO}_2 \text{ g}^{-1} \text{ N s}^{-1}$). Units of E_0 and R_x were unaffected. In the following text, we identify the results from the two different formulations (LAI versus canopy N predictors) as the LAI-model and the N-model.

(e) Parameter estimation and model evaluation

The NEE model was fit to the data by nonlinear regression, minimizing the root mean square error (r.m.s.e.) of predictions using the Excel SOLVER tool (Microsoft Office Excel 2010). We used as input data either the complete dataset (4853 simultaneous observations of NEE, air temperature and PAR, and estimates of LAI or N_T), or we used various subsets of the data. In the initial runs, the model-estimated parameters were R_0 , β , R_x , $P_{\max L}$, k and E_0 . However, as with our previous analysis of the 2003–2005 data from Toolik and Abisko [9], after numerous runs using different data subsets, we found that the model-estimated value of the light extinction coefficient, k , was unstable and often unrealistic (e.g. $k > 1$ or < 0). To eliminate this instability, we fixed the value of k at an ecologically realistic value of $0.5 \text{ m}^2 \text{ m}^{-2}$, leaving only R_0 , β , R_x , $P_{\max L}$ and E_0 to be estimated by the regression. Detailed explanation and justification for this procedure is provided in Shaver *et al.* [9].

Model parameters were calculated by regression using values of LAI (or N_T) estimated from NDVI measured in each plot, and measured air temperature (or soil temperature), PAR and NEE. The regression was performed on the entire dataset ('All data') and on data subsets. Subsets included data collected in all high Arctic sites, all low Arctic sites and individual sites and subsites (table 1). The resulting regression parameters were then used to predict NEE for the whole dataset and for individual sites and subsites. In other words, we used regression parameters derived from surveys of NEE in one part of the Arctic to predict NEE in other parts of the Arctic, and compared the accuracy of those predictions with predictions based on other parameter sets. The fit and accuracy of the model was assessed by comparing per cent variance explained (r^2) and r.m.s.e. of measured versus predicted NEE.

3. Results and discussion

(a) Overall and site-by-site regression results

When the entire dataset was used to estimate model parameters, the overall regression explained greater than 75 per cent of the variance in the data ($r^2 = 0.759$) with a r.m.s.e. of $1.51 \mu\text{mol CO}_2 \text{ m}^{-2} \text{ s}^{-1}$ (figure 1 and table 2). This result is quite similar to our previous analysis of the smaller dataset from Toolik and Abisko ($n = 1444$, $r^2 = 0.799$, r.m.s.e. = 1.53). For comparison, a r.m.s.e. of $1.5 \mu\text{mol m}^{-2} \text{ s}^{-1}$ is approximately two to three times the underlying methodological error associated with each measurement using this method [8], and it is less than 7 per cent of the overall range of measured NEE values.

The model parameters derived from the entire dataset were also ecologically reasonable. For example, $P_{\max L}$ was $15.184 \mu\text{mol CO}_2 \text{ m}^{-2} \text{ s}^{-1}$, at the high end of the range of P_{\max} values reported for individual leaves at Toolik Lake and Imnavait Creek [23,24]. The value of β , $0.046^{\circ}\text{C}^{-1}$, indicated a Q_{10} for respiration of approximately 1.58, which is also reasonable for cold, often waterlogged tundra soils and associated vegetation [25,26]. The quantum yield, $E_0 = 0.041 \mu\text{mol CO}_2 \mu\text{mol PAR}^{-1}$, is consistent with a canopy with generally low leaf area and low sun angle.

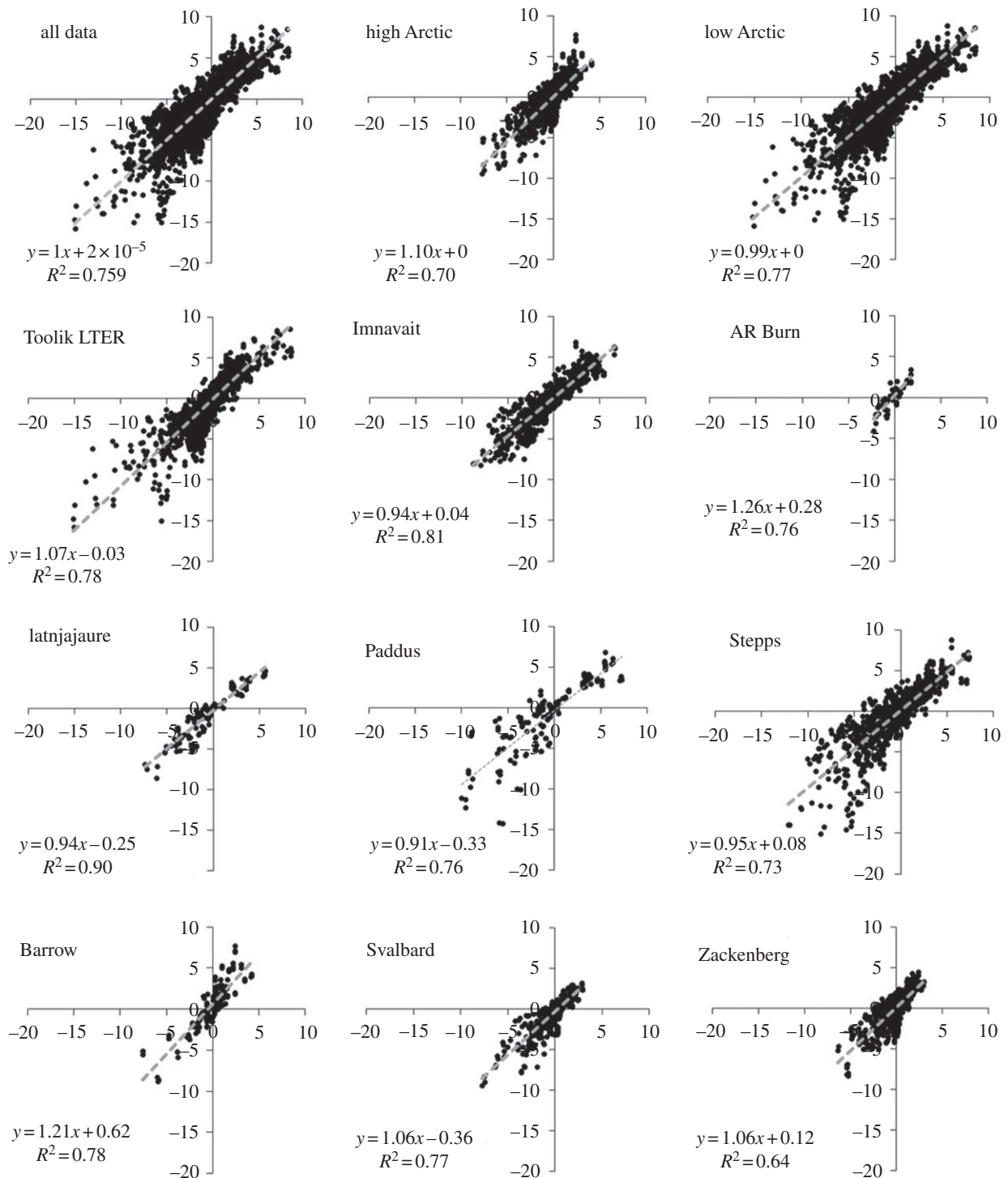


Figure 1. Predicted versus measured NEE using the entire dataset ('all data') in the regression to determine model parameters. Predicted values of NEE using these 'all data' regression parameters are plotted on the horizontal axes, with measured values on the vertical axes. Units of both axes are $\mu\text{mol CO}_2 \text{ m}^{-2} \text{ s}^{-1}$. The upper left plot includes all 4834 predicted and measured values; other plots include predicted and measured values within the various data subsets (table 2). The trend-line, equation and r^2 value in each plot describe the correlation between predicted and measured values within each data subset.

When the model parameters were estimated using smaller subsets of the data (table 2), the per cent variance explained was also consistently high (74–93%). R.m.s.e. was often lower for these site-by-site regressions than for the regression using the entire dataset, but r.m.s.e. ranged from 0.42 to 2.14 $\mu\text{mol CO}_2 \text{ m}^{-2} \text{ s}^{-1}$ depending on site. Parameter values for the individual site regressions varied considerably, however, especially for the P_{maxL} and β parameters (table 2). For all three of the high Arctic sites, P_{maxL} was greater than 20 $\mu\text{mol m}^{-2} \text{ s}^{-1}$, and for Barrow, P_{maxL} as estimated by regression was greater than 150 $\mu\text{mol m}^{-2} \text{ s}^{-1}$. For the AR Burn site, P_{maxL} was greater than 46 $\mu\text{mol m}^{-2} \text{ s}^{-1}$. These values for P_{maxL} are unlikely to

be accurate as they are much greater than measured values for leaf-level photosynthesis in the dominant species at these sites [23,24]. Similarly, the range of predicted values for β , and thus Q_{10} , indicated a range of Q_{10} from less than 1.5 to greater than 3.3, with a maximum of 15.6 in the AR Burn site. Values of $Q_{10} > 3.0$ have not been reported before for respiration of Arctic plants or soils during the growing season although very high 'apparent' Q_{10} has been reported for CO_2 releases from under snow cover [25,26]. Thus, although the model fits the data quite well for every data subset, occasionally it did so with biologically unreasonable parameter values. In the most extreme case, the regression using data from the AR Burn site

Table 2. Model parameters and statistics of fit (r^2) and accuracy (r.m.s.e.) for regressions using the entire dataset and data subsets. In these regressions, the k parameter was fixed at 0.500 in all cases.

datasets and subsets	n	model parameters, statistics and units							
		$P_{\max L}$ $\mu\text{mol CO}_2$ m^{-2} leaf s^{-1}	E_0 $\mu\text{mol CO}_2$ μmol^{-1} PAR	β $^{\circ}\text{C}^{-1}$	R_0 $\mu\text{mol CO}_2 \text{ C}$ m^{-2} leaf s^{-1}	R_x $\mu\text{mol CO}_2 \text{ m}^{-2}$ ground s^{-1}	Q_{10} $^{\circ}\text{C}^{-1}$	r^2	r.m.s.e. $\mu\text{mol CO}_2 \text{ m}^{-2}$ ground s^{-1}
all data	4853	15.184	0.041	0.046	1.233	0.729	1.59	0.759	1.510
high Arctic	1179	20.532	0.037	0.071	1.313	0.381	2.03	0.739	1.161
Longyearbyen	473	20.746	0.036	0.778	0.120	0.000	3.32	0.801	0.949
Zackenbergl	549	25.945	0.029	1.974	0.058	0.285	1.78	0.705	1.163
Barrow	157	156.988	0.016	0.252	0.115	1.216	3.15	0.740	1.470
low Arctic	3674	14.747	0.041	0.046	1.177	0.803	1.59	0.769	1.580
Abisko	1372	13.350	0.043	0.838	0.058	0.889	1.79	0.749	1.746
Latnjajaure	119	16.855	0.030	1.624	0.029	0.551	1.34	0.906	0.923
Paddus	148	14.342	0.035	0.430	0.083	0.572	2.30	0.873	2.138
Stepps	1105	13.080	0.047	0.844	0.061	0.922	1.84	0.738	1.735
Toolik Lake	2250	15.716	0.041	1.476	0.039	0.723	1.48	0.789	1.469
Imnavait	679	15.615	0.035	0.400	0.092	0.805	2.21	0.821	1.269
LTER	1571	16.119	0.044	1.743	0.034	0.729	1.40	0.786	1.517
AR Burn	52	46.864	0.031	0.035	0.275	0.856	15.62	0.931	0.420

Table 3. Statistics of fit (r^2) and accuracy (r.m.s.e.) for predictions of NEE based on regression parameters derived from the entire dataset, for high Arctic data only, and for the low Arctic data only. Numbers in bold represent cells where NEE is predicted for the same dataset used for model parametrization. Numbers in plain font represent cells where parameters derived by regression using one dataset are used to predict NEE in a different dataset.

data used in regression	n	datasets predicted by regression parameters					
		r^2 , predicted versus observed			r.m.s.e., predicted versus observed		
		all data	high Arctic	low Arctic	all data	high Arctic	low Arctic
all data	4853	0.759	0.703	0.769	1.512	1.258	1.585
high Arctic	1179	0.622	0.739	0.627	2.192	1.167	2.431
low Arctic	3674	0.759	0.698	0.769	1.513	1.271	1.583

had the highest r^2 and lowest r.m.s.e. among all regressions, but this was based on completely unreasonable estimates of both $P_{\max L}$ and β (table 2).

The unreasonable values of $P_{\max L}$ and β in some of the site-level regressions (table 2) were all found when using data subsets where the overall range of measurements of NEE was narrower than in other data subsets and especially when few measurements were available from high light and/or high temperature conditions. In all four cases where the site-by-site regressions gave values of $P_{\max L} > 20$, there were few if any measurements made at PAR values greater than $600 \mu\text{mol photons m}^{-2} \text{s}^{-1}$ and thus there were few if any NEE values less than $-7 \mu\text{mol CO}_2 \text{ m}^{-2} \text{s}^{-1}$ (figure 1). Three of these were at the high Arctic sites, Longyearbyen, Zackenberg and Barrow, where incoming PAR is always low due to low sun angles and frequent cloudiness, and the fourth was at the AR Burn site, where all 3 days of measurement were cloudy. As a result, in these four data subsets, the regression was insufficiently constrained by measurements made at or near light-saturating conditions, and $P_{\max L}$ is an extrapolated value far outside the range of measurements. Similarly, the high values of β ($Q_{10} > 3.0$) were all for data subsets where the overall range of air temperatures and NEE measurements was less than for other data subsets. The highest Q_{10} values were at the AR Burn site and at Barrow and Longyearbyen where the overall range of observed NEE was only approximately $10 \mu\text{mol C m}^{-2} \text{s}^{-1}$ or less (figure 1).

Although regressions based on the different data subsets produce a wide range of parameter values (table 2), parameters estimated in the regression using the entire dataset can be used to make accurate predictions of NEE at all of the individual sites and subsites. When measured values of NEE for individual sites were compared with predicted NEE using regression parameters derived from the whole dataset, the model did about equally well at predicting NEE at each site (figure 1). Regression slopes of measured versus predicted values were close to 1.0 for all sites, with intercepts not significantly different from zero. Per cent variance explained for data from individual sites ranged from 64 per cent at Zackenberg to 90 per cent at Latnjajaure. R.m.s.e. (not shown in figure 1) varied from approximately $0.9 \mu\text{mol CO}_2 \text{ m}^{-2} \text{s}^{-1}$ at the AR Burn to $2.2 \mu\text{mol CO}_2 \text{ m}^{-2} \text{s}^{-1}$ at Paddus.

(b) High Arctic versus low Arctic

When data from the high Arctic were used to estimate model parameters, the regression explained 73.9 per cent

of the variance in NEE in the high Arctic dataset, a small improvement over the use of parameters derived from the entire dataset to predict NEE in the high Arctic (70.3% in figure 1 and table 3). The r.m.s.e. for measured versus modelled NEE in the high Arctic data was $1.17 \mu\text{mol CO}_2 \text{ m}^{-2} \text{s}^{-1}$, also a small improvement over the r.m.s.e. of $1.26 \mu\text{mol m}^{-2} \text{s}^{-1}$ when NEE in the high Arctic was predicted using parameters derived from the entire dataset. The parameter values, though, were considerably different in the regression using high Arctic data only, with a much higher $P_{\max L}$ ($20.53 \mu\text{mol m}^{-2} \text{s}^{-1}$), a higher value of β (0.071, equivalent to a Q_{10} of 2.03), a slightly lower E_0 (0.037) and higher R_0 and lower R_x (table 2).

When the parameters developed from the high Arctic data were used to predict NEE in the low Arctic, or in the entire dataset, the variance explained in these other datasets was considerably lower, only 62–63 per cent (table 3). R.m.s.e. was also much higher, greater than $2 \mu\text{mol CO}_2 \text{ m}^{-2} \text{s}^{-1}$. By contrast, when data from the low Arctic were used to estimate model parameters, the parameter values were similar to the values derived using the whole dataset. This result is in part due to the fact that the low Arctic dataset is about three times larger than the high Arctic dataset, comprising about three-fourths of total data available. More importantly, though, parameters derived from the low Arctic data led to predictions of NEE in the high Arctic that explained almost 70 per cent of variation in the high Arctic dataset (table 3). When low Arctic parameters were used to predict high Arctic NEE, the r.m.s.e. was even lower (1.27) than when low Arctic parameters were used to predict low Arctic NEE (r.m.s.e. = 1.58).

The different parameter values derived for the high Arctic data might be explained in part as local adaptations to cooler climate with lower PAR. For example, a higher Q_{10} might be expected in colder environments of the high Arctic [27], although Q_{10} values this high have never been reported for Arctic ecosystems. Changes in leaf N and leaf area–leaf N relationships might be partly responsible for the higher $P_{\max L}$ in the high Arctic [14,28]. However, one key difference between the low and high Arctic datasets is that the high Arctic data include a much narrower range of observed values of NEE, LAI, PAR and air temperature on which the regression is based. For the high Arctic sites, there are very few NEE values greater than 5.0 or less than $-6.0 \mu\text{mol m}^{-2} \text{s}^{-1}$ (figure 1), and very few observations when GPP was close to saturation [14]. What this means for the present analysis is that predictions of NEE in the low Arctic based on parameters

derived from the high Arctic are extrapolations, whereas predictions of NEE in the high Arctic based on parameters derived from the low Arctic are interpolations.

The main reason for the high values of $P_{\max L}$ and β in the high Arctic regression (table 2) is the lack of measurements at high light or high temperatures to better constrain the regression at its extremes. One way to achieve this constraint is to fix one or both of these parameters at more reasonable values, letting the regression procedure solve for the remaining parameters as we did in fixing the value of k in table 2. For example, we repeated the analysis in table 3, but with the value of β fixed at 0.046 (the same value calculated for the regression including the whole dataset). The results (table 4) indicate an improvement in variance explained and a further reduction in r.m.s.e. when high Arctic data were used to predict NEE in the low Arctic or in the entire dataset. The value of $P_{\max L}$ for the high Arctic regression was still higher than expected at almost $20 \mu\text{mol CO}_2 \text{ m}^{-2} \text{ s}^{-1}$, though. It is possible that this high predicted value of $P_{\max L}$ actually reflects higher leaf level rates of light-saturated photosynthesis in high Arctic plants. However, most Arctic species have leaf-level P_{\max} values less than $20 \mu\text{mol CO}_2 \text{ m}^{-2} \text{ s}^{-1}$ [23,24]. To achieve a canopy-level P_{\max} ($=P_{\max L}$ in this model) of less than $20 \mu\text{mol CO}_2 \text{ m}^{-2} \text{ leaf s}^{-1}$, the average high Arctic vegetation canopy would have to be composed mostly of species with unusually high leaf-level P_{\max} and all of the individual leaves in the canopy would have to be arranged so that they are fully illuminated at high incoming PAR; this is extremely unlikely. High Arctic plants do have slightly higher average leaf N content [14], which might support higher potential rates of light-saturated photosynthesis, but in reality, the available light levels in these high latitudes are rarely if ever high enough to achieve these rates. Thus, we interpret these high $P_{\max L}$ values as artefacts resulting from a lack of observations of NEE at high PAR in these datasets to constrain these regression-derived parameters. Fixing the value of $P_{\max L}$ at a more reasonable value of $14\text{--}15 \mu\text{mol m}^{-2} \text{ s}^{-1}$ in regression using the high Arctic dataset results in predictions that are very similar to those using either the low Arctic dataset or the entire dataset (results not shown).

(c) Low Arctic versus high Arctic with net ecosystem exchange as a function of N_T

When NEE was predicted as a function of canopy N content (N_T) rather than LAI, the % variance explained was further increased and the r.m.s.e. was further reduced ($r^2=0.770$, r.m.s.e. = 1.476 in the 'all data' regression; table 5). The N-model parameters indicate a $P_{\max L}$ of $8\text{--}10 \mu\text{mol CO}_2 \text{ g}^{-1} \text{ canopy N s}^{-1}$, with a lower quantum yield than in the analyses based on LAI. The R_0 parameter varied from 0.6 to $1.0 \mu\text{mol CO}_2 \text{ g}^{-1} \text{ canopy N s}^{-1}$. Although the units of $P_{\max L}$ and R_0 in these regressions were different when N_T rather than LAI was used, the ratios of these two parameters stayed about the same; $P_{\max L}$ was always approximately 10–12 times the value of R_0 no matter what the units were (table 4 versus table 5). Similarly, $P_{\max L}$ and R_0 varied among the various data subsets in about the same way, with higher values when using the high Arctic data and lower values for the low Arctic and for all data. When using N_T to predict NEE, the value of R_x was consistently higher, by approximately $0.2\text{--}0.35 \mu\text{mol CO}_2 \text{ m}^{-2} \text{ s}^{-1}$, than when LAI was

used although the values of R_x changed in the same way among the data subsets.

The similarities in the relationships among the model parameters using either N_T or LAI to predict NEE for different datasets are almost certainly due to the overall close correlation between N_T and LAI, which appears in all of the individual data subsets as well as the overall dataset [13,29]. We also know that the vertical distribution of N in the canopy differs from the vertical distribution of leaf area (i.e. N concentration is not constant at all canopy heights; [14]), which may explain the relatively small differences in calculated quantum efficiency using N_T versus LAI. The slightly higher values of R_x when using N_T to predict NEE may be due to the functioning of this term as essentially a remainder in the regression calculation [9].

(d) Effect of using soil versus air temperature to predict net ecosystem exchange

Using soil temperature at 5 cm instead of air temperature to predict NEE led to *less* accurate predictions (larger r.m.s.e.) and poorer fit of predictions to measurements (lower r^2) although these regressions still explained at least 67 per cent of the variance in the data in all comparisons, with r.m.s.e. always less than $1.9 \mu\text{mol CO}_2 \text{ m}^{-2} \text{ s}^{-2}$ (table 5). There are at least two likely reasons for this: first, R_0 , the temperature-controlled component of R_E , was assumed to include both above-ground and below-ground plant respiration as well as soil respiration. Although one might expect above-ground plant respiration to be correlated with below-ground soil temperatures, the actual range of above-ground temperatures experienced during the measurement of NEE was much greater than the range of below-ground temperatures. One might expect that above-ground plant respiration would be more closely related to this greater variation in air temperatures than to the variation in soil temperatures. Second, there may be a time lag between the effect of soil temperature variation on soil and root respiration and the measurement of that change in respiration using our cuvette method, due to the time it takes for CO_2 to diffuse through the soil and into the well-mixed air volume of the cuvette. These problems could be solved by increasing the complexity of the model to include separate above-ground and below-ground biomass pools and temperature controls, but this would add at least one new parameter and one more variable to the model; it would require measurement of both soil and air temperature for every measurement of NEE. For the purposes of this study, the remarkable fact is how little difference it makes using either soil or air temperature to predict NEE.

4. Conclusions

Our primary conclusion is that a single parametrization of a single regression model can be used to explain most of the fine-scale, short-term variation in NEE of CO_2 throughout the Arctic, including both high and low Arctic (figure 1, $r^2=0.759$). Thus, it is reasonable to model short-term changes in the C balance of the entire Arctic as if it were a single ecosystem, with similar responses to variation in temperature, PAR and LAI throughout the region. Because our dataset was dominated by measurements made mostly between mid-July and early August, the accuracy of the

Table 4. Model parameters and statistics of fit and accuracy for regressions using the entire dataset and for high and low Arctic data only. In these regressions, the k parameter was fixed at 0.500 and the β parameter was fixed at 0.046. (a) Regression parameters. (b) Statistics of fit (r^2) and accuracy (r.m.s.e.) for predictions of NEE based on regression parameters for all data and for high Arctic and low Arctic data subsets. Numbers in bold represent cells where NEE is predicted for the same dataset or subset used for model parametrization. Numbers in plain font represent cells where parameters derived by regression using one dataset are used to predict NEE in a different dataset.

$P_{\max L}$		E_0	R_0	R_x	Q_{10}
data used in regression		$\mu\text{mol CO}_2 \text{ m}^{-2} \text{ leaf s}^{-1}$	$\mu\text{mol CO}_2 \mu\text{mol}^{-1} \text{ PAR}$	$\mu\text{mol CO}_2 \text{ m}^{-2} \text{ ground s}^{-1}$	$^{\circ}\text{C}^{-1}$
(a) model parameters and units					
all data	15.183	0.041	1.234	0.728	1.585
high Arctic	19.808	0.040	2.160	0.279	1.585
low Arctic	14.747	0.041	1.177	0.803	1.585
R^2 , predicted versus observed					
data used in regression		n	high Arctic	low Arctic	all data
(b) datasets predicted by regression parameters					
all data	4853	0.759	0.703	0.769	1.512 1.258 1.585
high Arctic	1179	0.697	0.732	0.704	1.857 1.184 2.027
low Arctic	3674	0.759	0.698	0.769	1.513 1.271 1.583

Table 5. Canopy N content, PAR and air temperature used to predict NEE. Note, change in units of P_{\max} and R_0 from tables 2–4 and 6. (a) Regression parameters for fit of all data and for high and low Arctic data subsets to the NEE model, with k fixed at 0.500 and β fixed at 0.046. In these regressions, the k parameter was fixed at 0.500 and the β parameter was fixed at 0.046. (b) Statistics of fit (r^2) and accuracy (r.m.s.e.) for predictions of NEE based on regression parameters for all data and for high Arctic and low Arctic data subsets. Numbers in bold represent cells where NEE is predicted for the same dataset or subset used for model parametrization. Numbers in plain font represent cells where parameters derived by regression using one dataset are used to predict NEE in a different dataset.

		P_{\max}	E_0	R_0	R_x	Q_{10}
data used in regression		$\mu\text{mol CO}_2 \text{ g}^{-1} \text{ canopy N s}^{-1}$	$\mu\text{mol CO}_2 \mu\text{mol}^{-1} \text{ PAR}$	$\mu\text{mol CO}_2 \text{ g}^{-1} \text{ canopy N s}^{-1}$	$\mu\text{mol CO}_2 \text{ m}^{-2} \text{ ground s}^{-1}$	$^{\circ}\text{C}^{-1}$
(a) model parameters and units						
all data		8.182	0.028	0.608	1.049	1.584
high Arctic		9.987	0.023	1.024	0.439	1.584
low Arctic		7.999	0.029	0.581	1.152	1.584
R^2 , predicted versus observed						
data used in regression		n	all data	high Arctic	low Arctic	all data
(b) datasets predicted by regression parameters						
all data		4853	0.770	0.715	0.779	1.476 1.221 1.548
high Arctic		1179	0.708	0.745	0.712	1.765 1.155 1.921
low Arctic		3674	0.770	0.709	0.779	1.477 1.234 1.547
r.m.s.e.						

Table 6. LAI, PAR and soil temperature (NOT air temperature) used to predict NEE. (a) Regression parameters for fit of all data and for high and low Arctic data subsets to the NEE model, with k fixed at 0.500 and β fixed at 0.046. (b) Statistics of fit (r^2) and accuracy (r.m.s.e.) for predictions of NEE based on regression parameters for all data and for high Arctic and low Arctic data subsets. Numbers in bold represent cells where NEE is predicted for the same dataset or subset used for model parametrization. Numbers in plain font represent cells where parameters derived by regression using one dataset are used to predict NEE in a different dataset.

		$P_{\max L}$	E_0	R_0	R_x	Q_{10}
data used in regression		$\mu\text{mol CO}_2 \text{ m}^{-2} \text{ leaf s}^{-1}$	$\mu\text{mol CO}_2 \mu\text{mol}^{-1} \text{ PAR}$	$\mu\text{mol CO}_2 \text{ m}^{-2} \text{ leaf s}^{-1}$	$\mu\text{mol CO}_2 \text{ m}^{-2} \text{ ground s}^{-1}$	$^{\circ}\text{C}^{-1}$
(a) model parameters and units						
all data		13.741	0.042	2.604	0.609	1.585
high Arctic		18.917	0.038	3.282	0.334	1.585
low Arctic		13.272	0.042	2.435	0.773	1.585
R^2 , predicted versus observed						
data used in regression		n	all data	high Arctic	low Arctic	all data
(b) datasets predicted by regression parameters						
all data		4480	0.722	0.675	0.734	1.634
high Arctic		1179	0.714	0.682	0.723	1.725
low Arctic		3301	0.722	0.672	0.735	1.638
						1.722
						1.344
						1.288
						1.857
						1.722

predictions of NEE will also be greatest in mid-season. All of the measurements in the dataset were made at the scale of a small plot, $\leq 1 \text{ m}^2$, with NEE changing in a time scale of 0–30 s. We showed previously, though, that the same model can be used to make accurate predictions of *daily* variation in NEE in the summertime over areas approximately 1 km^2 in the low Arctic, using satellite-based estimates of NDVI-LAI and NEE measured at eddy covariance towers [10]. Results of the present analysis indicate that the same upscaling procedures could be used to predict NEE on a daily basis, over areas of 1 km^2 and perhaps larger, anywhere in the Arctic. Longer-term predictions will require additional information, in particular, on the controls over leaf area and how it changes on a seasonal basis and from year to year.

Second, we have shown that the dataset used to estimate model parameters and to predict NEE does not need to include measurements from the same site or even from the same kind of Arctic ecosystem where NEE is predicted. All that is needed to generate appropriate parameters is a sufficiently broad survey of local variation in ecosystem properties, including measurements made at extreme values of LAI, PAR and temperature, and thus both high and low values of NEE; this is particularly important to properly constrain the model's estimates of P_{maxL} and β . The r.m.s.e. of predictions made in this way is at least as low (lower r.m.s.e. \approx more accurate), and sometimes lower, than predictions made using data collected at the same site where NEE is predicted. In the particular example used here, model parameters generated from surveys of NEE, LAI, PAR and air temperature at low Arctic sites led to predictions of NEE at high Arctic sites that were little different from predictions based on high Arctic data. The reverse was not true, however: because the high Arctic data covered a narrower range of NEE, PAR, LAI and air temperature, predictions of low Arctic NEE based on parameters developed from the high Arctic dataset were extrapolations, not interpolations, with much higher r.m.s.e. and less explanatory power than when low Arctic data were used to generate regression parameters.

Third, in a test of alternative variables as predictors of NEE, we show that canopy N content can be substituted for LAI in predicting NEE, with slightly higher per cent variance explained and slightly greater accuracy (lower r.m.s.e.). Although this is not surprising given the close correlation between canopy N content and LAI that we have observed throughout the Arctic [14,16,29], the fact that N content is a slightly better predictor than LAI is largely due to the close link between tissue N concentration, photosynthetic capacity and leaf respiration. By contrast, substituting soil temperature for air temperature in the model leads to predictions of NEE that are slightly less accurate and less successful at explaining variance in NEE. The reason for this is twofold: firstly that soil temperature is less variable and changes more slowly than air temperature during the period of measurement, and secondly that above-ground plant respiration is a major component of R_E that should be more closely linked to air temperature. There may also be a time lag between a change in soil temperature and the measurement of its effect on NEE, due to the time required for CO_2 to diffuse through soil. On the other hand, soil and air temperatures are also strongly correlated with each other, leading to similar predictions of NEE when either is used as a predictor.

With only about 25 per cent of the total variance in NEE left unexplained, further improvements in the present model

are likely to be small. Much of this unexplained variance is probably associated with inherent errors of the cuvette method of measurement of CO_2 flux, equal to 30–50 per cent of the r.m.s.e. of model predictions of approximately $1.5 \mu\text{mol CO}_2 \text{ m}^{-2} \text{ s}^{-1}$ [8]. Another significant portion is probably due to errors in the estimation of LAI. As we have shown previously, the use of NDVI to estimate LAI leads to overestimates when species with pubescent, silvery leaves (several species of *Salix*) are present [9] or when the background is extremely dark as in recently burned tundra [30]. We also underestimate LAI when the canopy includes a high proportion of closely appressed, overlapping leaves, especially *Cassiope tetragona* [31]. Finally, our estimate of LAI assumes that mosses do not contribute to the photosynthetic surface area despite the important contributions of moss photosynthesis to NEE [32,33]. Most of these errors in estimation of leaf area would vary in relation to species composition, and thus would appear as 'species effects' on estimates of NEE.

Several kinds of improvements would require adding new parameters and/or new continuous or categorical variables to the model. Cahoon *et al.* [34] recently showed, for example, that categorical treatment of woodiness of the vegetation (woody versus non-woody) and soil temperature regime ('warm' versus 'cold') explained a significant portion of the variation in R_E along a latitudinal transect of Arctic and subarctic ecosystems, in addition to the dominant effect of temperature on R_E . As noted above, separation of R_E into above-ground versus below-ground and/or plant versus soil components, each with separate temperature and/or moisture controls, may also improve model predictions. We have shown previously that estimates of the GPP component of NEE can be improved by using separate NDVI-LAI regressions for different species or vegetation types [13], and we have also found that latitudinal changes in canopy N allocation and leaf area–N relationships have significant effects on GPP [14]. We know that mosses and lichens contribute significantly to GPP in Arctic tundras [32,33], but the present model uses an estimate of vascular leaf area (LAI) to estimate GPP. All of these known relationships could be added to the model and would improve its ability to explain variance in NEE. The main disadvantage of doing so is that it would require much greater effort in collecting the data needed to parametrize the model, including additional field sampling at all of the sites where NEE is to be predicted. This would confound one of the major advantages of the current model, which presently requires as inputs only variables (LAI, PAR and air temperature) that can be measured or estimated remotely.

As we have noted previously, it is remarkable that such diverse kinds of Arctic ecosystems, dominated by very different plant functional types, have apparently been shaped by the Arctic environment so that an overall measure of ecosystem function like NEE can be described in a single parametrization of a single model [9]. The success of this model at predicting NEE independently of any information on species composition, using either leaf area or whole-canopy N content, indicates a high level of convergence in canopy structure and function, and in plot-scale, short-term control of ecosystem C cycling throughout the Arctic.

Acknowledgement. We are particularly grateful for field support provided by Toolik Field Station, Zackenberg Ecological Research Station, UNIS-Svalbard and Abisko Natural Science Research Station.

References

- Chapin III FS. 2006 Reconciling carbon-cycle concepts, terminology, and methods. *Ecosystems* **9**, 1041–1050. (doi:10.1007/s10021-005-0105-7)
- Jonasson S, Chapin III FS, Shaver GR. 2001 Biogeochemistry in the Arctic: patterns, processes, and controls. In *Global biogeochemical cycles in the climate system* (eds E-D Schulze, SP Harrison, M Heimann, EA Holland, JJ Lloyd, IC Prentice, D Schimel), pp. 139–150. New York, NY: Academic Press.
- Walker MD, Daniels FJA, van der Maarel E (eds) 1994 Special feature: circumpolar Arctic vegetation. *J. Veg. Sci.* **5**, 757–920. (doi:10.1111/j.1654-1103.1994.tb00395.x)
- CAVM Team. 2003 Circumpolar Arctic Vegetation Map. (1:7,500,000 scale), Conservation of Arctic Flora and Fauna (CAFF) Map no. 1. U.S. Fish and Wildlife Service, Anchorage, AK, USA.
- McGuire AD *et al.* 2009 Sensitivity of the carbon cycle in the Arctic to climate change. *Ecol. Monogr.* **79**, 523–555. (doi:10.1890/08-2025.1)
- Sitch S *et al.* 2007 Assessing the carbon balance of circumpolar Arctic tundra using remote sensing and process modeling. *Ecol. Appl.* **17**, 213–234. (doi:10.1890/1051-0761(2007)017[0213:ATCBOC]2.0.CO;2)
- McGuire AD *et al.* 2012 An assessment of the carbon balance of Arctic tundra: comparisons among observations, process models, and atmospheric inversions. *Biogeosciences* **9**, 3185–3204. (doi:10.5194/bg-9-3185-2012)
- Williams M, Street LE, van Wijk M, Shaver GR. 2006 Identifying differences in rates of carbon exchange among vegetation types along an Arctic topequence. *Ecosystems* **9**, 288–304. (doi:10.1007/s10021-005-0146-y)
- Shaver GR, Street LE, Rastetter EB, van Wijk MT, Williams M. 2007 Functional convergence in regulation of net CO₂ flux in heterogeneous tundra landscapes in Alaska and Sweden. *J. Ecol.* **95**, 802–817. (doi:10.1111/j.1365-2745.2007.01259.x)
- Lorant MM, Goetz SJ, Rastetter EB, Rocha AV, Shaver GR, Humphreys ER, Lafleur PM. 2010 Scaling an instantaneous model of tundra NEE to the Arctic landscape. *Ecosystems* **14**, 76–93. (doi:10.1007/s10021-010-9396-4)
- Reich PB, Kloeppel BD, Ellsworth DS, Walters MB. 1995 Different photosynthesis–nitrogen relations in deciduous hardwood and evergreen coniferous tree species. *Oecologia* **104**, 24–30. (doi:10.1007/BF00365558)
- Davidson EA, Janssens IA. 2006 Temperature sensitivity of soil carbon decomposition and feedbacks to climate change. *Nature* **440**, 165–173. (doi:10.1038/nature04514)
- Street LE, Shaver GR, Williams M, van Wijk MT. 2007 What is the relationship between changes in leaf area and changes in photosynthetic CO₂ flux in Arctic ecosystems? *J. Ecol.* **95**, 139–150. (doi:10.1111/j.1365-2745.2006.01187.x)
- Street L, Shaver GR, Rastetter E, Van Wijk MT, Kaye B, Williams M. 2012 Incident radiation and the allocation of nitrogen within Arctic plant canopies: implications for predicting gross primary productivity. *Glob. Change Biol.* **18**, 2838–2852. (doi:10.1111/j.1365-2486.2012.02754.x)
- Van Wijk MT, Williams M. 2005 Optical instruments for measuring leaf area index in low vegetation: application in Arctic ecosystems. *Ecol. Appl.* **15**, 1462–1470. (doi:10.1890/03-5354)
- Williams M, Rastetter EB. 1999 Vegetation characteristics and primary productivity along an Arctic transect: implications for scaling up. *J. Ecol.* **87**, 885–898. (doi:10.1046/j.1365-2745.1999.00404.x)
- Shaver G *et al.* In press. Terrestrial ecosystems. In *A changing Arctic: ecological consequences of climate change for tundra, streams, and lakes* (eds JE Hobbie, GW Kling), ch. 5. Oxford, UK: Oxford University Press.
- Reynolds JF, Tenhunen JD (eds) 1996 *Landscape function and disturbance in Arctic tundra*. Springer-Verlag Ecological Studies Series, 110, p. 437. Berlin, Germany: Springer.
- Jones BM, Kolden CA, Jandt R, Abatzoglou JT, Urban F, Arp CD. 2009 Fire behavior, weather, and burn severity of the 2007 Anaktuvuk River Tundra Fire, North Slope, Alaska. *Arc. Antarct. Alp. Res.* **3**, 309–316. (doi:10.1657/1938-4246-41.3.309)
- Rocha A, Shaver GR. 2011 Burn severity influences post-fire CO₂ exchange in Arctic tundra. *Ecol. Appl.* **21**, 477–489. (doi:10.1890/10-0255.1)
- Bret Harte MS, Mack MC, Shaver GR, Huebner DC, Johnston M, Mojica CA, Pizano MC, Reiskind JA. 2013 The response of Arctic vegetation and soils following an unusually severe tundra fire. *Trans. R. Soc. B* **368**, 20120490. (doi:10.1098/rstb.2012.0490)
- Rastetter EB, King AW, Cosby BJ, Hornberger GM, O'Neil RV, Hobbie JE. 1992 Aggregating fine-scale ecological knowledge to model coarser-scale attributes of ecosystems. *Ecol. Appl.* **2**, 55–70. (doi:10.2307/1941889)
- Oberbauer SF, Oechel WC. 1989 Maximum CO₂ assimilation rates of vascular plants on an Alaskan Arctic tundra slope. *Holarctic Ecol.* **12**, 312–316.
- Chapin III FS, Shaver GR. 1996 Physiological and growth responses of Arctic plants to a field experiment simulating climatic change. *Ecology* **77**, 822–840. (doi:10.2307/2265504)
- Schimel JP, Fahnestock J, Michaelson G, Mikan C, Ping C-L, Romanovsky VE, Welker J. 2006 Cold-season production of CO₂ in Arctic soils: can laboratory and field estimates be reconciled through a simple modeling approach? *Arc. Antarct. Alp. Res.* **38**, 249–256. (doi:10.1657/1523-0430(2006)38[249:CPOCIA]2.0.CO;2)
- van de Weg MJ, Fetcher N, Shaver G. In press. Response of dark respiration to temperature in *Eriophorum vaginatum* from a 30-year-old transplant experiment in Alaska. *Plant Ecol. Divers.* (doi:10.1080/17550874.2012.729618)
- Atkin OK, Tjoelker MG. 2003 Thermal acclimation and the dynamic response of plant respiration to temperature. *Trends Plant Sci.* **8**, 343. (doi:10.1016/S1360-1385(03)00136-5)
- Kerkhoff AJ, Enquist BJ, Elser JL, Fagan WF. 2005 Plant allometry, stoichiometry, and the temperature-dependence of primary productivity. *Glob. Ecol. Biogeogr.* **14**, 585–598. (doi:10.1111/j.1466-822X.2005.00187.x)
- van Wijk M, Williams M, Shaver GR. 2005 Tight coupling between leaf area index and foliage N content in Arctic plant communities. *Oecologia* **142**, 421–427. (doi:10.1007/s00442-004-1733-x)
- Rocha AV, Shaver GR. 2009 Advantages of a two band EVI calculated from solar and photosynthetically active radiation fluxes. *Agr. For. Meteorol.* **149**, 1560–1563. (doi:10.1016/j.agrformet.2009.03.016)
- Campoli M, Street LE, Michelsen A, Shaver GR, Maere T, Samson R, Lemeur R. 2009 Determination of leaf area index, foliar N, and normalized difference vegetation index for Arctic ecosystems dominated by *Cassiope tetragona*. *Arc. Antarct. Alp. Res.* **41**, 426–433. (doi:10.1657/1938-4246-41.4.426)
- Douma JC, van Wijk MT, Shaver GR. 2007 The contribution of mosses to the carbon and water exchange of Arctic ecosystems: quantification and relationships with system properties. *Plant Cell Environ.* **30**, 1205–1215. (doi:10.1111/j.1365-3040.2007.01697.x)
- Street L, Stoy P, Sommerkorn M, Fletcher B, Sloan V, Hill TC, Williams M. 2012 Seasonal bryophyte productivity in the sub-Arctic: a comparison with vascular plants. *Funct. Ecol.* **26**, 365–378. (doi:10.1111/j.1365-2435.2011.01954.x)
- Cahoon SMP, Sullivan PF, Shaver GR, Welker JM, Post E. 2012 Interactions among shrub cover and the soil microclimate may determine future Arctic carbon budgets. *Ecol. Lett.* **15**, 1415–1422. (doi:10.1111/j.1461-0248.2012.01865.x)